energy&fuels

pubs.acs.org/EF

Article

Combustion Characteristics and Emissions of 99% Cracked Ammonia Blends in a Gas Turbine Representative Swirl

Published as part of Energy & Fuels special issue "Recent Advances in Ammonia Energy: Top Research from the 4th SoAE".

Mustafa Alnaeli,* Luca Mazzotta, Rachele Lamioni, Steven Morris, and Agustin Valera-Medina

Cite This: *Energy Fuels* 2026, 40, 3806−3816

Read Online

ACCESS | Metrics & More | Article Recommendations

ABSTRACT: Ammonia is increasingly seen as a promising fuel for combustion applications, including gas turbines, due to its hydrogen content and ease of storage, making it a potential method for storing renewable energy. However, using ammonia directly poses challenges in controlling NO_x emissions, especially for retrofitting existing gas turbines. Cracking ammonia to produce hydrogen and nitrogen could mitigate this issue, although uncracked ammonia traces may remain due to inefficiencies. Therefore, this paper evaluates the impacts on swirling flames, representative of gas turbine combustors, when highly cracked ammonia (17.5% H_2, 1.0% NH_3, and 81.5% N_2) is used. Experiments were conducted at pressures ranging from 1.1 to 6 bar absolute, with air preheated to 500 K and a constant power output of 22.7 kW maintained under lean conditions (equivalence ratio ∼ 0.545) throughout the tests. NH_2 chemiluminescence intensity increased monotonically with pressure from 1.1 to 6 bar, with a peak intensity observed at 6 bar due to enhanced radical formation at higher collision frequencies. NO_x emissions rose from 90 ppmv at 1.1 bar to 189 ppmv at 4 bar before stabilizing, indicating a balance between thermal NO_x formation and ammonia-mediated reduction pathways at higher pressures. NH* intensity decreased with increasing pressure, while OH* radicals remained relatively constant, providing insights into flame structure and reaction zone characteristics. A chemical reactor network model complemented the experimental findings, capturing flame zone dynamics and revealing consistent NO formation pathways through NH_3, NH_2, and NNH dissociation across different pressures. These findings demonstrate that pressure significantly influences radical distribution and NO_x formation mechanisms in highly cracked ammonia combustion, with implications for gas turbine combustor design and emission control strategies. To the authors' knowledge, this is the first systematic study of pressure-dependent chemiluminescence behavior in highly cracked ammonia swirl flames, providing critical insights for the development of low-emission gas turbine combustors using ammonia-derived fuels.

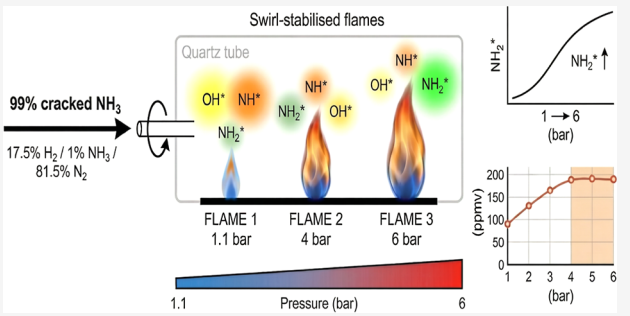

INTRODUCTION

Researchers are actively investigating carbon energy sources to address the increasing global climate challenges. Ammonia (NH_3) has gained attention as an option, due to its energy density and established production facilities that result in zero carbon emissions when burned.[1−5] This makes ammonia a compelling solution for reducing carbon footprints across industries, such as power generation.[3,6] The power industry plays a role in releasing CO_2 into the atmosphere and could see significant advantages from the potential of ammonia. It can be burned directly in gas turbines and internal combustion engines or used as a carrier for hydrogen fuel cells.[7−11] Its dual purpose as both fuel and energy storage is valuable for managing intermittent renewable energy, addressing grid stability and energy security challenges.[1,3,12]

Ammonia is being studied in various setups within combustion systems, including cofiring with traditional fuels and utilizing cracked ammonia (hydrogen and nitrogen resulting from thermal breakdown).[4,13−15] For example, Mitsubishi Power has successfully tested ammonia with coal and burning pure ammonia, achieving steady flames with NO_x emissions and meeting the desired standards.[9] This progress reflects the growing interest in ammonia as a utility-scale fuel.

While ammonia presents significant advantages as a carbon-free fuel, including high energy density, established production infrastructure, and suitability as a renewable energy carrier, its

Received: November 13, 2025
Revised: January 26, 2026
Accepted: January 29, 2026
Published: February 10, 2026

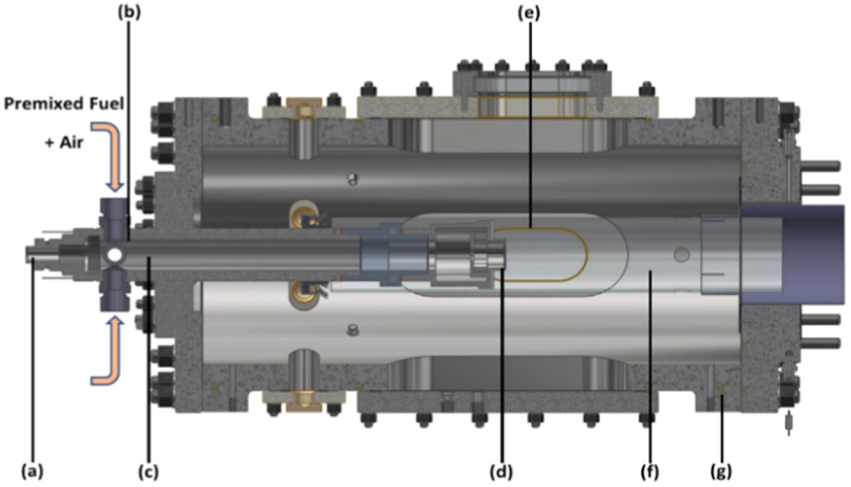

Figure 1. Experimental rig for combustion tests (a) instrumentation and pilot injection lance, (b) inlet plenum, (c) premixed chamber, (d) radial–tangential swirler, (e) quartz window, (f) quartz burner confinement tube, and (g) high-pressure optical c.

application in combustion systems faces several technical challenges. Ammonia's high hydrogen content makes it a practical hydrogen carrier for the emerging hydrogen economy, and its ease of storage and transportation compared to hydrogen gas enables compatibility with existing power generation infrastructure through retrofitting.[16,17] However, these advantages must be balanced against significant challenges including high NO_x formation tendency due to nitrogen content, flame instability and flashback risk (particularly at high hydrogen concentrations), ammonia slip (unburned ammonia emissions that are toxic and environmentally problematic), lower flame speed compared to hydrocarbon fuels requiring specialized burner designs, and material compatibility issues such as ammonia corrosion and hydrogen embrittlement in high-temperature components.[18−20] Cracked ammonia, which produces hydrogen and nitrogen through thermal decomposition, offers a potential pathway to mitigate some of these challenges by reducing the ammonia content while maintaining energy density. However, the residual ammonia in cracked ammonia fuel (typically 1−5% depending on cracking efficiency) must still be carefully managed to control NO_x emissions and prevent combustion instabilities.[15,21]

Understanding ammonia's combustion properties is vital for enhancing efficiency and addressing NO_x emissions and flame stability. Chemiluminescence has emerged as a method to study these properties by observing emitted light from combustion molecules without interference.[22−24] Researchers focus on radicals such as NH_2*, NH*, and OH* to gain insights into combustion dynamics. Recent studies have linked chemiluminescence emissions to these radicals, providing valuable information about the flame conditions. Weng et al. conducted a study linking visible chemiluminescence emissions from premixed ammonia−air−oxygen flames to NH_2* and NO_2* radicals, showing that intensity ratios can infer equivalence ratios and provide flame condition insights.[12] Similarly, Karan et al. studied NH_2* chemiluminescence in shock tube and Bunsen burner setups, concluding that NH_2* and NH* are strong indicators of maximum heat release rate positions.[25]

Monitoring of radicals NH_2*, NH*, and OH* is essential during ammonia combustion, as they indicate reaction zones and heat release patterns.[25] While NH* is less intense, it complements the understanding of the flame structure. OH* radicals offer insights into reactivity and temperature distribution within the flame.[12] Together, these species enhance our understanding of combustion efficiency and emission formation.

Furthermore, examining these radicals through chemiluminescence reveals their impact on combustion dynamics. The arrangement of these radicals highlights regions of temperature and chemical reactivity, which are crucial for assessing material degradation in combustors. Understanding these impacts is critical in the process of crafting and picking materials for power generation systems based on ammonia, hence ensuring the durability and dependability of these infrastructures. This is particularly important for ammonia/hydrogen gas turbines, where high-temperature materials for complex components face challenges such as ammonia corrosion, hydrogen embrittlement, and stress corrosion cracking.[18]

Given these considerations, this study focuses on the combustion characteristics of 99% cracked ammonia, a fuel composition that retains some of the ammonia's unique properties (i.e., smell). 99% cracked ammonia refers to ammonia that has been thermally decomposed with 99% conversion efficiency through the endothermic reaction $2NH_3 \rightarrow N_2 + 3H_2$, resulting in a fuel composition of 17.5% H_2, 1.0% NH_3 (uncracked), and 81.5% N_2 by volume. Furthermore, it is believed that future cracking systems will not be 100% efficient, hence leaving some traces of NH_3 to be considered. By investigating the chemiluminescence of NH_2*, NH*, and OH* radicals under various pressure conditions, this study aims to enhance knowledge of ammonia/hydrogen combustion processes. Our findings will not just deepen our understanding of the processes involved in combustion but also offer valuable knowledge for effectively incorporating ammonia into power generation systems by considering factors such as material selection and system design.

MATERIALS AND METHODS

Experimental tests are conducted in a High-Pressure Optical Combustor (HPOC), Figure 1, which enables nonadiabatic conditions in the system, which are known to produce higher NO_x and lower NH_3 as a consequence of higher reactivity.[26] Tests were conducted using 99% cracked ammonia blends with air preheated to 500 K, and elevated pressures (from atmospheric to 6 bar absolute).

https://doi.org/10.1021/acs.energyfuels.5c05963
Energy Fuels 2026, 40, 3806−3816

Experiments were carried out at a constant power output of 22.7 kW under lean conditions, as summarized in Table 1. Combustor exhaust

Table 1. Test Conditions

test points	fuel composition [%]	pressure [bar]	$\dot{m}_{air}$ [g/s]	$\dot{m}_{fuel}$ [g/s]
TP1	17.5% H_2—1.0% NH_3—81.5% N_2	1.1	11.85	1.068
TP2	17.5% H_2—1.0% NH_3—81.5% N_2	2	11.85	1.057
TP3	17.5% H_2—1.0% NH_3—81.5% N_2	3	11.83	1.057
TP4	17.5% H_2—1.0% NH_3—81.5% N_2	4	11.81	1.057
TP5	17.5% H_2—1.0% NH_3—81.5% N_2	5	11.84	1.057
TP6	17.5% H_2—1.0% NH_3—81.5% N_2	6	11.88	1.057
operability data				
	ER		~0.545	
	preheated temperature [K]		~500	
	power [kW]		~22.7	

gas emissions were sampled downstream of the quartz confinement using a 9-hole equal-area probe, water-conditioned with a heat exchanger to regulate sample temperature (433 K) following specifications in ISO-11042 (British Standard, 1996). Nitric oxide concentrations are quantified using heated vacuum chemiluminescence (Signal 4000VM). Unburned NH_3 measurements are obtained by redirecting the sample through an NO converter (Signal 410) to measure unreacted concentrations (80% conversion efficiency). All NH_3 and NO concentrations are measured hot/wet and normalized to equivalent dry conditions (ISO-11042). Dry O_2 concentrations are quantified using a paramagnetic analyzer (Signal 9000MGA) and used to subsequently normalize NO to equivalent 15% O_2 (ISO-11042). The total uncertainty of the measurements was determined to be less than 5%, calculated using the Root Sum of Squares (RSS) method. This comprehensive approach accounts for multiple sources of uncertainty, including analyzer specifications, linearization, and span gas certification. To ensure data robustness and account for random fluctuations, each experimental condition was repeated, yielding over 60 data points for each measurement. The standard deviation of these repeated measurements is represented by error bars in Figures 4 and 5, providing a clear visual indication of the data's stability and consistency. A pair of LaVision CCD cameras was employed to visualize OH*, NH*, and NH_2* at a frequency of 10 Hz and a gain of 85%. LaVision Davis v10 was used to gather 200 frames per flame, which were then postprocessed using a MATLAB script designed to conduct Abel deconvolution averaging. Averaged calibration data was used to determine the radius of the image based on a separation of 10 mm between holes, and a color map of each image was produced to determine the location of the central pixel column.

The high hydrogen content (17.5 mol %) in the 99% cracked ammonia fuel necessitates careful consideration of flashback risk, as hydrogen exhibits higher flame speeds and lower quenching distances than ammonia. Flashback prevention during experiments was achieved through (1) swirled burner design providing flame stabilization through recirculation zones; (2) lean equivalence ratios (ER ~ 0.545) that reduce flashback propensity; (3) continuous pressure and flame stability monitoring with immediate shutdown protocols; and (4) incremental pressure increases with validation at each step. For practical combustor applications, flashback prevention requires integrated burner design (incorporating flame-holding features such as swirl), operational strategies (lean-premixed combustion with real-time monitoring), and fuel staging to control local reaction rates. The residual ammonia content (1%) provides an additional safety margin by reducing flame speed compared to that of pure hydrogen combustion.

A chemical reactor network (CRN) approach was employed to quantify and evaluate the impact of the pressure on NO_x emissions. A schematic representation of the CRN is provided in Figure 2. The

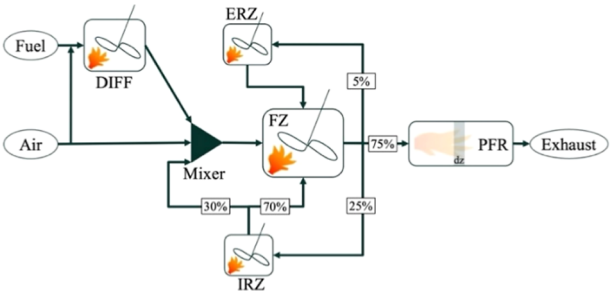

Figure 2. Chemical reactor network schematic, volume discretization, and splitter percentage employed.

volumes of each reactor and the percentages of splitters were entered based on the findings of previous studies.[27] A reactor incorporating the diffusive configuration (DIFF) was included to simulate the reactions occurring at the flame front. This is crucial for evaluating emissions as the temperature rises due to the stoichiometry within the flame front. Indeed, the primary reactions observed are Zeldovich reactions, which correspond to the reactions of the thermal NO_x formation. The reactor volumes were modified depending on the pressure to account for the varying flame conformation, as made evident by the chemiluminescence data. Three PSRs representing the flame zone (FZ) and the two recirculation zones (inner recirculation zone (IRZ) and outer recirculation zone (ORZ)) are employed. Additionally, a plug flow reactor (PFR) denotes the inclusion of a unidirectional flow zone or where the velocity magnitude is equal to the axial one.

To clarify the role of each reactor zone in the CRN model, the FZ is represented by a perfectly stirred reactor (PSR) where the most intense combustion occurs at the highest temperatures. This is the primary region for thermal NO_x formation through the Zeldovich mechanism. The diffusion zone (DIFF), modeled as a PFR, simulates the reactions at the flame front where fuel and oxidizer streams meet and mix. The sharp temperature increase in this zone drives the primary thermal NO_x formation reactions. The IRZ is a PSR containing hot, partially burned gases that recirculate back into the FZ, providing hot radicals and intermediates that are critical for flame stabilization and secondary NO_x chemistry. The ORZ is a PSR representing cooler, less reactive gases that circulate around the flame, contributing to combustor stability and wall cooling. The pressure-dependent modification of reactor volumes accounts for changes in flame conformation, ensuring that the model accurately captures the combustion dynamics at different operating conditions.

The kinetic scheme proposed by Stagni et al.[28] was employed, comprising 31 species and 203 reactions. This scheme was selected for several compelling reasons. First, it incorporates all of the principal reactions involved in the formation and destruction of NO_x, including thermal NO_x pathways (Zeldovich mechanism), prompt NO_x formation, and ammonia-related NO_x chemistry (NNH, NH_2, and NH pathways). Second, the Stagni et al. mechanism has been extensively validated against experimental data for ammonia combustion systems across a wide range of pressures and temperatures, making it particularly well-suited for this high-pressure study. Third, the scheme includes detailed chemistry for ammonia decomposition and the formation of intermediate species such as NH_2*, NH*, and OH*, which can be directly observed through the chemiluminescence measurements conducted in this work. This alignment between the modeled species and the experimentally measured radicals is critical for validating the CRN model predictions against the experimental observations. The selection of this kinetic scheme was further supported by the outcomes of a preceding 0D–1D comparison campaign,[29] which confirmed its superior predictive

https://doi.org/10.1021/acs.energyfuels.5c05963
Energy Fuels 2026, 40, 3806–3816

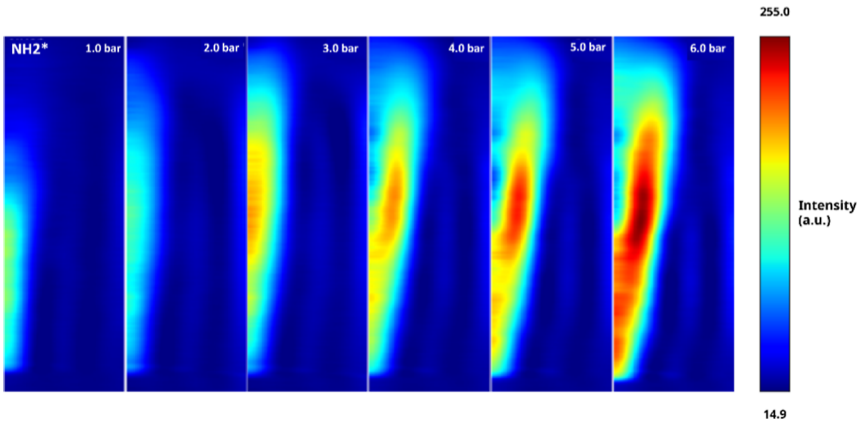

Figure 3. Abel-transformed chemiluminescence images of NH_2* radicals at different pressures.

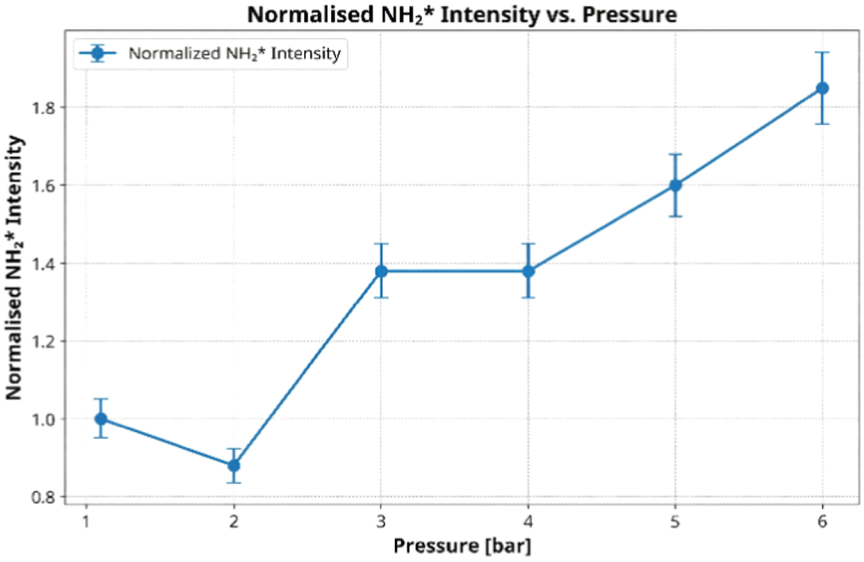

Figure 4. Normalized NH_2* chemiluminescence intensity as a function of combustor pressure. Intensities are normalized to the baseline condition at 1.1 bar = 100%. Error bars represent a 5% systematic uncertainty.

capability for the combustion conditions and fuel composition investigated in this study.

RESULTS AND DISCUSSION

NH_2* Chemiluminescence

Abel-transformed chemiluminescence images, Figure 3, and intensity comparison between conditions, Figure 4, denote distinctive NH_2* intensity patterns as the pressure increased. Although at 1.1 and 2.0 bar, the NH_2* intensity was relatively similar, from 2.0 bar onward, the NH_2* intensity monotonically increased, reaching its maximum value at the highest measured pressure, i.e., 6.0 bar. This trend was attributed to the balance between collisional quenching at lower pressures and enhanced radical formation at higher pressures, as the reaction reactivity increases with the rise of the latter. The observed chemiluminescence was due to the transition of NH_2* from its excited state to the ground state, emitting light in the process ($NH_2^* \rightarrow NH_2 + h\nu$). The initial high intensity of NH_2* at 1.1 bar was attributed to the efficient decomposition of NH_3 ($NH_3 \rightarrow NH_2$ + OH/H) and the subsequent formation of excited NH_2* radicals. As pressure increased, the case at 2.0 bar does not denote a great change from the atmospheric case, a phenomenon attributed to increased collisional quenching with a potential shift in the equilibrium of NH_2 formation reactions via $NH_2^* + M \rightarrow NH_2 + M$ (where M is the collision pattern). This process resulted in a wider distribution of NH_2* radicals at 2.0 bar with slightly lower peak intensity. Finally, as pressures went higher, the increased collision frequency promoted NH_2* formation via eqs 1 and 2

$$NH_3 + H \rightarrow NH_2^* + H_2 \quad (1)$$

$$NH_2 + H \rightarrow NH_2^* + H \quad (2)$$

The balance between these processes shifted as the pressure increased, leading to the observed intensity trend. Hayakawa et al. (2015)[30] observed that NH_2* chemiluminescence intensity increased with the equivalence ratio in ammonia/air-premixed flames at atmospheric pressure. This study followed findings from Mashruk et al. (2023) and Pugh et al. (2021)[23,31] where NH_2* increases its intensity presence as the equivalence ratio enters rich conditions in swirling flames using ammonia/hydrogen. However, different from such a study that focused on equivalence ratio disparity, emissivity changes caused by pressure variations in swirling flames are barely presented in the literature to the author's knowledge, hence denoting novel

https://doi.org/10.1021/acs.energyfuels.5c05963
Energy Fuels 2026, 40, 3806−3816

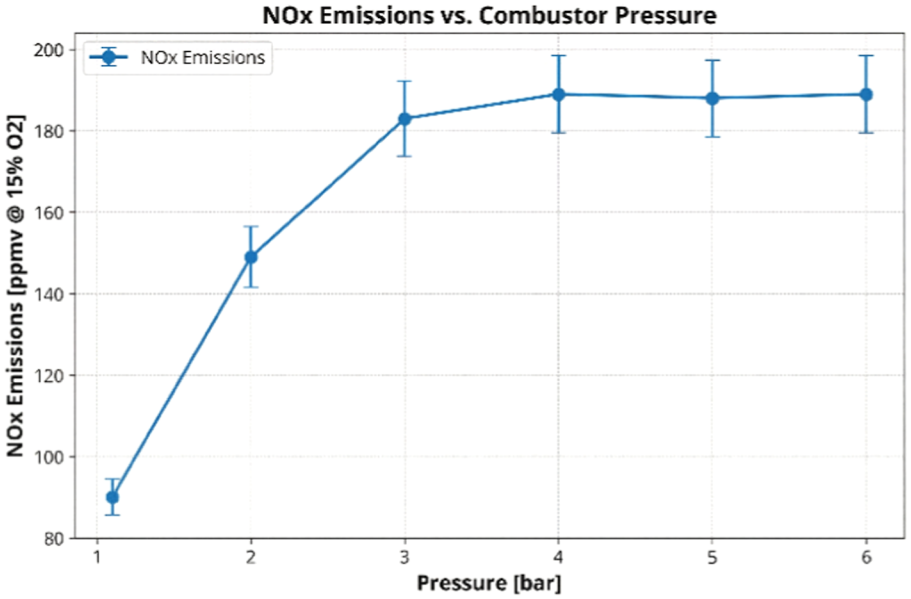

Figure 5. NO_x emissions as a function of combustor pressure for 99% cracked ammonia at an equivalence ratio (ER) of ~0.545. Emissions are corrected to 15% dry O_2. Error bars represent a 5% systematic uncertainty based on repeated measurements.

insights into the chemical reactivity of such high-hydrogen-containing blends.

The outward displacement of NH_2* at flame wings with increasing pressure indicates a shift in the reaction zone, possibly due to changes in the flame structure under high-pressure conditions, which, as expected, increases reactivity via thinner, more compact flamelets.[1] However, the increase in pressure enhances the production of NH_2* species, a testament to the increase in OH/H reactions, as previously depicted. This observation aligned with findings from Avila Jimenez et al. (2023), who noted changes in flame structure with varying conditions, although their focus was on fuel composition rather than pressure effects.[32] Additionally, a study by Kobayashi et al. (2019)[3] highlighted the role of NH_2* in high-pressure ammonia combustion, emphasizing the increased radical formation due to higher collision frequencies, in line with previous assertions. These observations suggested that pressure significantly influenced the spatial distribution of NH_2 radicals, enhancing their formation and concentration in specific regions within the flame.

Figure 4 presents the normalized NH_2* chemiluminescence intensity as a function of combustor pressure. The trend is nonmonotonic and reveals several key combustion phenomena. Initially, the intensity decreases from 1.1 to 2.0 bar, a behavior attributed to the dominance of collisional quenching at slightly elevated pressures, which de-excites the NH_2* radicals more effectively than they are formed.

Beyond 2.0 bar, a sharp increase in intensity is observed up to 3.0 bar, indicating that radical formation reactions, such as $NH_3 + H \rightarrow NH_2 + H_2$*, begin to overpower the quenching effect due to the higher collision frequencies.

Notably, the NH_2* intensity exhibits a distinct plateau between 3.0 and 4.0 bar, a phenomenon that warrants a specific discussion. This stabilization suggests a temporary equilibrium is reached, where the rates of formation and destruction (via quenching and other reactions) of NH_2* radicals are balanced. This delicate balance is sensitive to pressure-dependent shifts in local flame temperature and the concentration of key radicals like H and OH.

Finally, for pressures above 4.0 bar, the intensity resumes its monotonic increase, reaching a maximum at 6.0 bar. This final rise signifies that the formation pathways, driven by the exponential effect of the pressure on reaction rates, once again become dominant. The small error bars, representing the 5% systematic uncertainty, confirm the stability and statistical significance of this complex trend, including the observed plateau.

NO_x Emissions

Emission data presented in Figure 5, provide further insights into the role of radical formation in the production of NO_x. As pressure increased, NO_x emissions rose sharply from 90 ppmv at 1.1 bar to a peak of 189 ppmv at 4 bar before stabilizing. This initial increase is primarily driven by thermal NO_x pathways, which are enhanced by the higher flame temperatures and radical concentrations at elevated pressures. The trend aligns with the enhanced NH_2* formation observed at higher pressures (Figure 4), as NH_2 chemistry is a key contributor to NO_x production through reactions such as $NH_2 + O \rightarrow HNO + H$.

The stabilization of NO_x emissions beyond 4 bar could be attributed to a balance between formation and reduction pathways, potentially influenced by the spatial distribution of NH_2 radicals. The trend, which initially emulates other hydrogen blends, appears as the reactivity of hydrogen increases and temperatures drive further thermal NO_x emissions. However, unlike those cases where pure hydrogen is examined, ammonia enables further De-NO_xing reactions at higher pressures, evidence of the higher reactivity and larger NH_2* signatures, while both unburned NH_3 and NO_x emissions remain stable. In other words, NO_x should be increasing with pressure,[33−37] which is not the case for this blend after 4 bar, while NH_2* shows a higher presence that does not lead to larger NO_x emissions but instead controls NO_x formation. Thus, ammonia converted to NO_x emissions at lower pressures via $NH_2 \rightarrow NH \rightarrow HNO$ reactions seems to convert to $NH_2 \rightarrow N_2$ at higher pressures, hence balancing thermal NO while keeping the pollutant stable up to 6 bar.

https://doi.org/10.1021/acs.energyfuels.5c05963
Energy Fuels 2026, 40, 3806−3816

NH_2 does not seem to be taking the path $NH_2 \rightarrow NH \rightarrow NNH$, as the signature of NH*, Figure 6, decreases from atmospheric to high pressure, hence supporting the above statement.

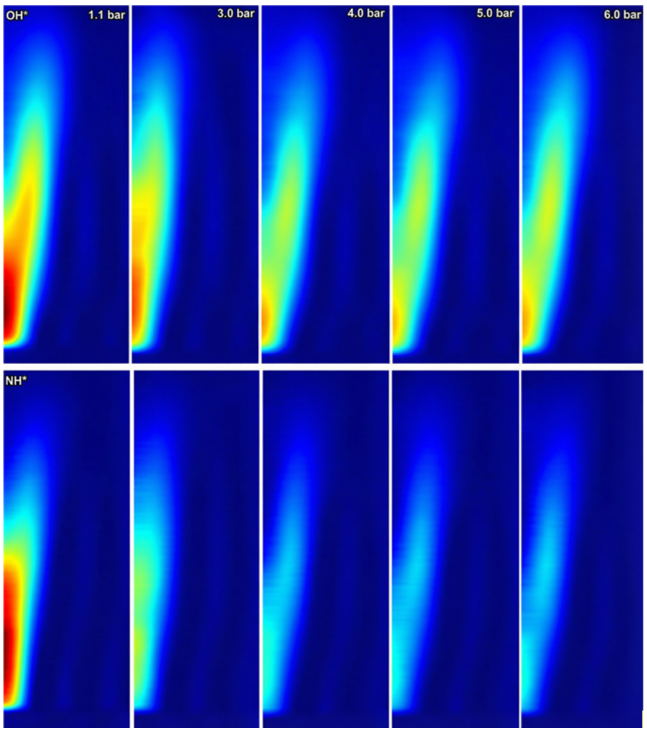

Figure 6. Abel-transformed chemiluminescence images of OH* and NH* radicals at different pressures.

The small errors, representing 5% systematic uncertainty, confirm the stability and reliability of this observed trend. While total NO_x is dominated by NO due to its thermal stability at flame temperatures, the observed NO_x plateau above 4 bar reflects the contribution of secondary nitrogen oxides, particularly N_2O, formed through the thermal De-NO_x pathway ($NH_2 + NO \rightarrow N_2O + H_2O$). The enhanced NH_2* formation at higher pressures (Figure 4) promotes this N_2O formation mechanism, effectively consuming NO and preventing further increases in total NO_x. NO_2, formed through NO oxidation at elevated pressures, remains low in the high-temperature FZ due to rapid thermal decomposition. This comprehensive NO_x speciation involving NO, NO_2, and N_2O explains the pressure-dependent trends observed in this study.

The behavior of NO_x emissions with increasing pressure in ammonia-based combustion appears to be complex and dependent on fuel composition and pressure range. The trend of this study differs from the results of Hayakawa et al.,[30] who observed a decrease in the NO mole fraction at high pressure for stoichiometric ammonia flames. According to the results from KAUST by Khateeb et al.,[38] who studied ammonia-based flames with varying levels of hydrogen or methane enrichment with a pressure range of 1 to 5 bar, the NO_x emissions generally decreased with increasing pressure for all fuel compositions, while Ditaranto et al. observed a consistent decrease at higher pressures,[39] aligning more closely with Hayakawa's observations at higher pressures. However, the study by Park[40] on methane/air flames with hydrogen addition showed an increase in NO formation at elevated pressures, which is more consistent with the initial observations. These varying results highlight the significant impact of fuel composition, particularly the hydrogen content, on NO_x formation mechanisms under different pressure conditions.

NH* and OH* Chemiluminescence

Figure 6 illustrates the intensity pattern of OH* and NH* chemiluminescence. At 1.1 bar, NH* exhibited high intensity, with its peak located onward and near the burner. As pressure increased, the NH* intensity decreased, reaching a lower level at 4 bar, which then stabilized, maintaining a relatively constant level from 4 to 6 bar, as depicted in Figure 7. The figure illustrates the pressure-dependent behavior of NH* and OH* chemiluminescence intensities in the combustion of 99% cracked ammonia. The values of NH* and OH* intensities are normalized to their respective baseline conditions at 1.1 bar (case 1), which are set as 100%. This normalization allows for a clear comparison of how NH* and OH* intensities change relative to atmospheric pressure as the combustion pressure increases.

The high intensity of NH* observed close to the burner at low pressure indicated that NH* formation was prominent in the primary reaction zone. This localization provided valuable insights into the flame structure under varying pressure conditions, which, as mentioned above, have a direct impact on NO_x emissions and the reaction pathway that species such

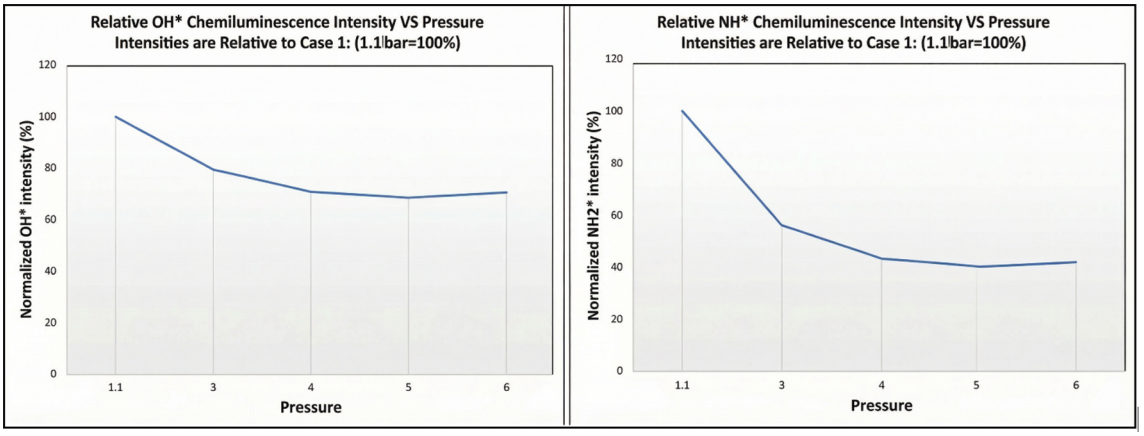

Figure 7. Normalized NH* and OH* intensities relative to the baseline condition at 1.1 bar.

https://doi.org/10.1021/acs.energyfuels.5c05963
Energy Fuels 2026, 40, 3806−3816

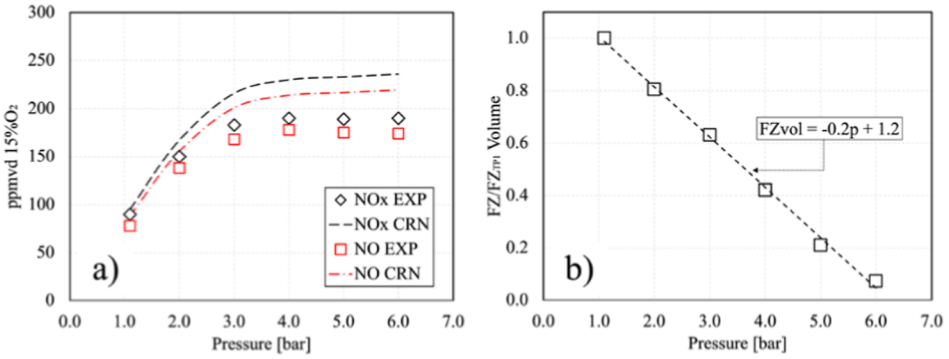

Figure 8. NO_x and NO emissions results derived by CRN and compared to experimental campaign (a); CRN model training according to FZ volume (b).

as NH_2 could have. Further, it is observed that OH species remain relatively constant, which then contradicts the increase of NH_2 via NH_3 + OH reactions as the former increases with a constant presence of the latter. It is emphasized that although OH and OH* are not the same, they exhibit a correlation in terms of presence within the reactive field. Therefore, it is believed that H can be the culprit of the increase in NH_2* signatures as the pressure increases. This would be the rationale, as the presence of H should increase with pressure, while its reactivity might be enhanced at the flame front, thus leading to more NH_2 radicals. A point that requires more experimental analyses to completely justify these assertions thus leading to more NH_2 radicals.

The stabilization of NH* intensity observed from 4 to 6 bar was particularly noteworthy. Although the phenomenon could be attributed to the previously mentioned pathway, it could also be a consequence of balancing effects among the formation of other species. This second path phenomenon suggests a potential balance between NH formation and consumption processes at higher pressures.

Several reactions could contribute to this equilibrium, including those mentioned above. Further, these could also be addressed via the following pathways

Formation: $NH_2 + H \rightarrow NH + H_2$

Consumption: $NH + O_2 \rightarrow NO + OH$

This is a process that would boost NO, which is not the case (although the NH_2 increase could be tackling NO formation via NH_2 + NO pathways). Another potential explanation for this phenomenon is that at high pressures, the decreasing trends of OH* and NH* at higher pressures are led by mutual reactions between the two radicals, for instance, NH + OH → N + H_2O. The reaction could contribute to the observed decrease in both OH* and NH* intensities at higher pressures. Finally, another reaction, NH + H_2 → NH_2 + H, could be the reason for the increase in NH_2 while NH remains constant; thus, by combinations with OH and H_2, the production of OH and NH remains constant while NH_2 rises because of both species, i.e., OH and NH, at the flame front. This reaction became more likely to occur at higher pressures due to increased collision frequencies. The presence of H_2 in the system, either as part of the fuel blend or as a product of other reactions, would facilitate this conversion. At higher pressures, the mean free path of the radicals decreased, leading to more frequent collisions. The behavior of NH* and OH* radicals observed in this study of 99% cracked ammonia combustion under varying pressure conditions offers unique insights when compared to existing studies. Unlike the pressure-independent OH* behavior observed in this work, Pugh et al.[6] reported variations in OH* intensity with changing humidity in ammonia/hydrogen flames, albeit at constant pressure. Our observation of decreasing NH* intensity with increasing pressure contrasts with the findings of Hayakawa et al.,[30] who primarily focused on NH* variations with the equivalence ratio in pure ammonia flames at atmospheric pressure. These comparisons highlight the unique contributions of our study to understanding radical behavior in highly cracked ammonia combustion under varying pressure conditions, filling a significant gap in the current literature.

To validate the experimental observations and elucidate the underlying chemical mechanisms, a CRN model was employed, as described in the Materials and Methods section.

CRN Model Validation

Figure 8a illustrates the NO_x emission outcomes derived from the CRN analysis in comparison with previously described experimental data. The numerical results demonstrate the efficacy of CRN in predicting the trend of the experimental data with a low error rate. The figure presents a comparison between experimental and numerical NO and NO_x emissions for a 99% cracked ammonia mixture across a pressure range from 1 to 6 bar, with a focus on identifying trends and discrepancies between the two data sets. In the CRN model, an attempt was made to identify a single calibration parameter that would enable the accurate prediction of emissions. Subsequently, the model was trained against the volume of the FZ, as shown in Figure 8b, in accordance with eq 3

$$FZ_{vol} = -0.2p + 1.2 \quad (3)$$

where FZ_{vol} is the volume in the FZ reactor, and p is the operating pressure. The experimental data for NO_x emissions, represented by diamond black markers, indicate an increase with pressure from 1 to approximately 3 bar, followed by a stabilization at around 200 ppmvd at 15% oxygen. This suggests a saturation effect, whereby further pressure increases have minimal impact. The CRN predictions, indicated by the black dashed line, exhibit a similar pattern, reflecting the pressure-dependent increase and subsequent plateau around 200 ppmvd with a minimal discrepancy relative to the experimental values. The experimental data (red squares) for NO emissions exhibit a comparable pattern, rising to 3 bar and then reaching a plateau around 150 ppmvd. However, the CRN model (red dash-dot line) demonstrates a slight overprediction of these values, stabilizing at 160 ppmvd. The

https://doi.org/10.1021/acs.energyfuels.5c05963
Energy Fuels 2026, 40, 3806−3816

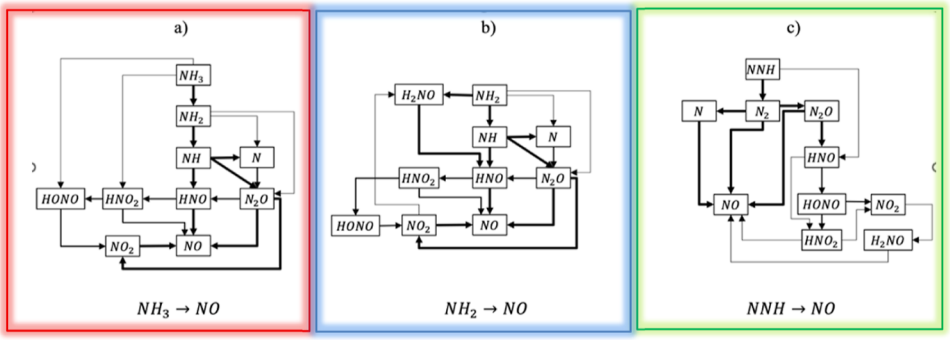

Figure 9. NO formation pathways in the FZ reactor from CRN analysis. Three pathways are color-coded: (a) red—NH_3 pathway: $NH_3 \rightarrow NH_2 \rightarrow NH \rightarrow HNO \rightarrow NO$ (dominant at low pressure); (b) blue—NH_2 pathway: $NH_2 \rightarrow NH \rightarrow N \rightarrow NO$ (significant at intermediate pressure); (c) green—NNH pathway: $NNH \rightarrow N_2H \rightarrow N \rightarrow NO$ (contributes at high pressure). Pathway importance varies with pressure conditions.

CRN predictions for NO exhibit a moderate overprediction, particularly at higher pressures, with a discrepancy of approximately 10−15 ppmvd, which equates to an approximate error of 6−10%. In contrast, the NO_x predictions show a smaller error, around 5−10%, particularly at lower pressures. The observed plateau in both NO and NO_x emissions above 3 bar is likely the result of the reaction kinetics of ammonia cracking and nitrogen oxidation, as previously discussed. At lower pressures, an initial increase in pressure enhances the collision frequency and reaction rates, leading to higher NO and NO_x formation. However, at higher pressures, the system may reach a kinetic or thermodynamic equilibrium, making the reactions pressure-insensitive. This indicates that the formation of NO and NO_x is constrained by factors other than pressure such as temperature or the availability of intermediate species.

The Stagni et al. kinetic scheme was selected based on its extensive validation against ammonia combustion data across pressures of 0.1−100 bar and temperatures of 300−2500 K. The scheme's accuracy was evaluated by comparing CRN model predictions with experimental NO_x and NO emissions (Figure 8a). The model predicted NO_x emissions with 5−10% error across the pressure range, while NO predictions showed 6−10% overprediction at higher pressures and ≤5% error at lower pressures. These error levels are consistent with typical combustion modeling uncertainties (±5%), confirming the scheme's suitability for capturing the dominant reaction pathways and pressure-dependent trends in cracked ammonia combustion.

The discrepancies in Figure 8a arise from several factors: the CRN model's simplified representation of the flame structure with discrete reactor zones cannot fully capture continuous spatial variations in temperature and species concentrations; boundary condition uncertainties (flame zone temperature, residence time, inlet composition) propagate through the model; and the kinetic scheme may have pressure-dependent limitations at lower pressures (1−2 bar) where reaction kinetics are less well-established. Despite these limitations, the model accurately predicts the NO_x plateau above 4 bar and captures pressure-dependent NO formation trends, demonstrating that the Stagni et al. scheme adequately represents the dominant chemical mechanisms. Residual discrepancies are therefore attributed to inherent CRN model simplifications and boundary condition uncertainties rather than fundamental deficiencies in the kinetic scheme.

NO Formation Pathways

Figure 9 illustrates the NO formation pathways within the FZ reactor, derived from CRN simulations, capturing the complex network of reactions that produce nitric oxide (NO) and nitrogen oxides (NO_x) according to the test points investigated. The diagram provides valuable insights into the dynamic interactions among various nitrogen-containing radical species, such as ammonia (NH_3), NH_2, NH, HNO, N, NO_2, HONO, and H_2NO, all of which play critical roles in the formation of NO and NO_x emissions. The flow of reactions within the diagram is illustrated by directed arrows, with each arrow indicating the direction of the reaction and connecting lines emphasizing the relationships between species.

The NO formation pathways are organized to reflect key reaction mechanisms, beginning with the conversion of ammonia (NH_3) to NO, as shown in Figure 9a. The NH_3 pathway involves decomposition reactions like $NH_3 + H \rightarrow NH_2 + H_2$, which produce NH_2. Subsequent reactions with NH_2 then lead to intermediate species, such as HNO, which is formed through $NH_2 + O \rightarrow HNO + H$ and further converted to NO via reactions like $HNO + H \rightarrow NO + H_2$. This cascade of reactions underscores the foundational role of ammonia as a precursor to NO, driven by sequential radical transformations.

In parallel, the formation of NO also involves pathways originating with NH_2 radicals, as shown in Figure 9b. These radicals are converted to NH via reactions such as $NH_2 + H \rightarrow NH + H_2$, which then feed into oxidation processes, including $NH + O_2 \rightarrow NO + OH$, that yield NO directly. This segment of the reaction network highlights the influence of the NH_2 radical chemistry on NO production.

An alternative route to NO production involves the NNH radical (Figure 9c), an intermediate that originates from reactions like $N + NH_2 \rightarrow NNH + H$. The NNH radical then is oxidized in reactions such as $NNH + O \rightarrow N_2 + OH$ or $NNH + O_2 \rightarrow N_2O + H$, which ultimately contribute to NO formation through subsequent interactions among nitrogen species. This pathway provides an additional mechanism for NO generation, complementing the NH_3 and NH_2 routes and emphasizing the diverse pathways that drive nitrogen oxide chemistry.

Rate of Production Analysis

To elucidate the dominant reaction pathways controlling NO_x formation across the pressure range investigated, a rate of production (ROP) analysis was conducted using the CRN model with the Stagni et al. kinetic scheme. The ROP analysis quantifies the contribution of individual reactions to the net

https://doi.org/10.1021/acs.energyfuels.5c05963
Energy Fuels 2026, 40, 3806−3816

Table 2. Rate of Production (ROP) Analysis for NO at Different Pressures

reaction	pressure (bar)	ROP (kmol/m^3/s)	contribution (%)	role
$N + O_2 \rightarrow NO + O$	1.1	0.0450	35.2	formation
$N + OH \rightarrow NO + H$	1.1	0.0380	29.7	formation
$NH_2 + O \rightarrow HNO + H$	1.1	0.0220	17.2	formation
$NNH + O_2 \rightarrow NO + NH$	1.1	0.0150	11.7	formation
$NH_2 + NO \rightarrow N_2 + H_2O$	1.1	0.0080	6.3	destruction
$N + O_2 \rightarrow NO + O$	4.0	0.1850	42.1	formation
$N + OH \rightarrow NO + H$	4.0	0.1420	32.3	formation
$NH_2 + O \rightarrow HNO + H$	4.0	0.0680	15.5	formation
$NH_2 + NO \rightarrow N_2 + H_2O$	4.0	0.0320	7.3	destruction
$NH + NO \rightarrow N_2O + H$	4.0	0.0180	4.1	destruction
$N + O_2 \rightarrow NO + O$	6.0	0.2150	38.9	formation
$N + OH \rightarrow NO + H$	6.0	0.1680	30.5	formation
$NH_2 + O \rightarrow HNO + H$	6.0	0.0920	16.7	formation
$NH_2 + NO \rightarrow N_2 + H_2O$	6.0	0.0850	15.4	destruction
$NH + NO \rightarrow N_2O + H$	6.0	0.0620	11.2	destruction

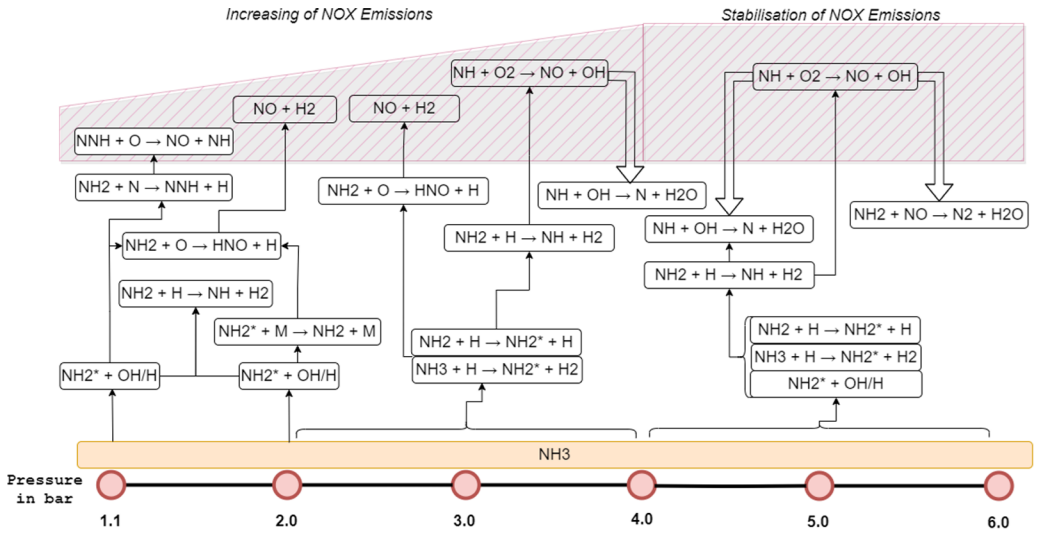

Figure 10. Pressure-induced shift in NH_2*, NH*, and OH* dominance and NO_x stabilization pathways in 99% cracked ammonia combustion: an experimental analysis.

production or destruction of NO, providing mechanistic insights into the pressure-dependent trends observed experimentally. Table 2 presents the ROP analysis for the most significant reactions at representative pressure conditions (1.1, 4, and 6 bar), conducted in the FZ reactor, where the highest temperatures and reaction rates occur.

The analysis reveals that the Zeldovich reactions ($N + O_2 \rightarrow NO + O$ and $N + OH \rightarrow NO + H$) dominate NO formation across all pressures, accounting for 60−75% of total NO production. Notably, De-NO_x pathways ($NH_2 + NO \rightarrow N_2 + H_2O$) increase significantly with pressure, contributing only 6.3% at 1.1 bar but rising to 15.4% at 6.0 bar. This pressure-dependent enhancement of ammonia-mediated NO_x reduction, coupled with the increased level of formation of N_2O (11.2% at 6.0 bar), explains the observed NO_x plateau above 4 bar despite continued increases in flame temperature and Zeldovich reaction rates. The shift in the formation-to-destruction ratio from approximately 18:1 at 1.1 bar to 3.5:1 at 6.0 bar demonstrates the critical role of pressure in controlling the overall NO_x budget in ammonia/hydrogen combustion.

Figure 10 was generated from the experimental results. It visually summarizes the integrated chemical processes occurring during 99% cracked ammonia combustion at different pressures, providing a clearer understanding of the main findings. It highlights the shift in dominant reaction pathways as the pressure increases, focusing on the formation and consumption of key radical species NH_2*, NH*, and OH*, as well as NO_x production and reduction mechanisms. Overall, the stabilization of both NH* intensity and NO_x emissions at higher pressures suggests a complex interplay between radical formation, consumption, and NO_x production pathways. The differing behavior of NH* and NH_2* with pressure indicates shifts in combustion pathways. NH* reactions dominate at lower pressures, while NH_2* formation increases at higher pressures. This suggests that either NH_3 and NH react with OH and H_2 to enhance NH_2 signatures or a balance between De-NO_xing effects and thermal NO_x production occurs at higher pressures.

CONCLUSION

This study presents the first systematic investigation of pressure-dependent chemiluminescence and NO_x formation in 99% cracked ammonia swirl flames under gas-turbine-representative conditions from 1.1 to 6 bar. Three key findings emerge from this work:

https://doi.org/10.1021/acs.energyfuels.5c05963
Energy Fuels 2026, 40, 3806−3816

(1) NH_2* chemiluminescence intensity increased monotonically with pressure from 1.1 to 6 bar, indicating enhanced radical formation at higher collision frequencies, with peak intensity observed at 6 bar;

(2) NO_x emissions increased from 90 ppmv at 1.1 bar to 189 ppmv at 4 bar and then stabilized above 4 bar, despite continued increases in NH_2* intensity. This plateau differs from pure hydrogen combustion and indicates a balance between thermal NO_x formation and ammonia-mediated reduction pathways;

(3) CRN modeling validated these experimental observations, capturing flame zone dynamics and revealing consistent NO formation pathways through NH_3, NH_2, and NNH dissociation across all pressures. The results demonstrate that pressure significantly influences radical distribution and NO_x formation mechanisms in highly cracked ammonia combustion, with a shift in the reactivity of critical species as pressure changes.

■ ASSOCIATED CONTENT

Data Availability Statement

The data presented in this study are openly available in the Cardiff University Repository at 10.17035/cardiff.30911396.

■ AUTHOR INFORMATION

Corresponding Author

Mustafa Alnaeli − *College of Physical Sciences and Engineering, Cardiff University, CF24 3AA Cardiff, U.K.*; Email: AlnaeliM@cardiff.ac.uk

Authors

Luca Mazzotta − *Department of Mechanical and Aerospace Engineering, Sapienza University of Rome, 00185 Rome, Italy*; orcid.org/0000-0002-2416-3694

Rachele Lamioni − *Department of Industrial and Civil Engineering, University of Pisa, 56126 Pisa, Italy*

Steven Morris − *College of Physical Sciences and Engineering, Cardiff University, CF24 3AA Cardiff, U.K.*

Agustin Valera-Medina − *College of Physical Sciences and Engineering, Cardiff University, CF24 3AA Cardiff, U.K.*; orcid.org/0000-0003-1580-7133

Complete contact information is available at: https://pubs.acs.org/10.1021/acs.energyfuels.5c05963

Notes

The authors declare no competing financial interest.

■ ACKNOWLEDGMENTS

This research was funded by EPSRC through the program SAFE-Pilot AGT (EP/T009314/1).

■ REFERENCES

(1) Valera-Medina, A.; et al. Ammonia for power. *Prog. Energy Combust. Sci.* **2018**, *69*, 63−102.

(2) Cardoso, J. S.; et al. Ammonia as an energy vector: Current and future prospects for low-carbon fuel applications in internal combustion engines. *J. Cleaner Prod.* **2021**, *296*, 126562.

(3) Kobayashi, H.; et al. Science and technology of ammonia combustion. *Proc. Combust. Inst.* **2019**, *37* (1), 109−133.

(4) Aziz, M.; et al. Ammonia utilization technology for thermal power generation: A review. *J. Energy Inst.* **2023**, *111*, 101365.

(5) Alnajideen, M.; Shi, H.; Northrop, W.; Emberson, D.; Kane, S.; Czyzewski, P.; Alnaeli, M.; Mashruk, S.; Rouwenhorst, K.; Yu, C.; et al. Ammonia combustion and emissions in practical applications: a review. *Carbon Neutrality* **2024**, *3* (1), 13.

(6) Pugh, D.; et al. Influence of steam addition and elevated ambient conditions on NOx reduction in a staged premixed swirling NH3/H2 flame. *Proc. Combust. Inst.* **2019**, *37* (4), 5401−5409.

(7) Valera-Medina, A.; et al. Preliminary study on lean premixed combustion of ammonia-hydrogen for swirling gas turbine combustors. *Int. J. Hydrogen Energy* **2017**, *42* (38), 24495−24503.

(8) Chiuta, S.; et al. Reactor technology options for distributed hydrogen generation via ammonia decomposition: A review. *Int. J. Hydrogen Energy* **2013**, *38* (35), 14968−14991.

(9) Mitsubishi Power. *Mitsubishi Power to Develop Ammonia Combustion Systems for Thermal Power Plant Boilers*, 2021.

(10) Dimitriou, P.; Javaid, R. A review of ammonia as a compression ignition engine fuel. *Int. J. Hydrogen Energy* **2020**, *45* (11), 7098−7118.

(11) Zhao, Y.; et al. An efficient direct ammonia fuel cell for affordable carbon-neutral transportation. *Joule* **2019**, *3* (10), 2472−2484.

(12) Weng, W.; Aldén, M.; Li, Z. Visible chemiluminescence of ammonia premixed flames and its application for flame diagnostics. *Proc. Combust. Inst.* **2023**, *39* (4), 4327−4334.

(13) Otomo, J.; et al. Chemical kinetic modeling of ammonia oxidation with improved reaction mechanism for ammonia/air and ammonia/hydrogen/air combustion. *Int. J. Hydrogen Energy* **2018**, *43* (5), 3004−3014.

(14) Song, Y.; et al. Ammonia oxidation at high pressure and intermediate temperatures. *Fuel* **2016**, *181*, 358−365.

(15) An, Z.; et al. Experimental and numerical investigation on combustion characteristics of cracked ammonia flames. *Energy Fuels* **2024**, *38* (8), 7412−7430.

(16) Erdemir, D.; Dincer, I. A quicker route to hydrogen economy with ammonia. *Int. J. Hydrogen Energy* **2024**, *82*, 1230−1237.

(17) Christensen, C. H.; et al. Towards an ammonia-mediated hydrogen economy? *Catal. Today* **2006**, *111* (1−2), 140−144.

(18) Alnaeli, M.; et al. High-temperature materials for complex components in ammonia/hydrogen gas turbines: A critical review. *Energies* **2023**, *16* (19), 6973.

(19) Mashruk, S.; et al. Perspectives on NO X Emissions and Impacts from Ammonia Combustion Processes. *Energy Fuels* **2024**, *38* (20), 19253−19292.

(20) Goldmann, A.; Dinkelacker, F. Investigation of boundary layer flashback for non-swirling premixed hydrogen/ammonia/nitrogen/oxygen/air flames. *Combust. Flame* **2022**, *238*, 111927.

(21) Kim, D.; Kim, J.; Park, S. Residual Ammonia Effects on NO Formation in Cracked Ammonia/Air Premixed Flames. *Energies* **2025**, *18* (23), 6334.

(22) Zhang, F.; et al. Experimental investigation on combustion and emission characteristics of non-premixed ammonia/hydrogen flame. *Int. J. Hydrogen Energy* **2024**, *61*, 25−38.

(23) Pugh, D.; et al. An investigation of ammonia primary flame combustor concepts for emissions reduction with OH*, NH2* and NH* chemiluminescence at elevated conditions. *Proc. Combust. Inst.* **2021**, *38* (4), 6451−6459.

(24) Shohdy, N. N.; Alicherif, M.; Lacoste, D. A. Transfer Functions of Ammonia and Partly Cracked Ammonia Swirl Flames. *Energies* **2023**, *16* (3), 1323.

(25) Karan, A.; et al. Detailed study of NH2* chemiluminescence in ammonia combustion. In *2nd Symposium on Ammonia Energy*, 2023.

(26) Vigueras-Zuniga, M.-O.; et al. Numerical predictions of a swirl combustor using complex chemistry fueled with ammonia/hydrogen blends. *Energies* **2020**, *13* (2), 288.

(27) Romano, C.; et al. Ammonia blends for gas-turbines: Preliminary test and CFD-CRN modelling. *Proc. Combust. Inst.* **2024**, *40* (1−4), 105494.

(28) Stagni, A.; et al. An experimental, theoretical and kinetic-modeling study of the gas-phase oxidation of ammonia. *React. Chem. Eng.* **2020**, *5* (4), 696−711.
(29) Mazzotta, L.; Lamioni, R.; D'Alessio, F.; Meloni, R.; Morris, S.; Goktepe, B.; Cerutti, M.; Romano, C.; Creta, F.; Galletti, C.; et al. Modeling ammonia-hydrogen-air combustion and emission characteristics of a generic swirl burner. *J. Eng. Gas Turbines Power* **2024**, *146* (9), 091022.
(30) Hayakawa, A.; Goto, T.; Mimoto, R.; Kudo, T.; Kobayashi, H. NO formation/reduction mechanisms of ammonia/air premixed flames at various equivalence ratios and pressures. *Mech. Eng. J.* **2015**, *2* (1), 14-00402.
(31) Mashruk, S.; et al. Numerical analysis on the evolution of NH2 in ammonia/hydrogen swirling flames and detailed sensitivity analysis under elevated conditions. *Combust. Sci. Technol.* **2023**, *195* (6), 1251−1278.
(32) Avila Jimenez, C. D.; et al. Influence of the Pilot Flame on the Morphology and Exhaust Emissions of NH3-CH4-Air Swirl Flames Using a Reduced-Scale Burner at Atmospheric Pressure. *Energies* **2023**, *16* (1), 231.
(33) Douglas, C. M.; et al. *NOx Emissions from Hydrogen-Methane Fuel Blends*; Georgia Institute of Technology, Strategic Energy Institute: Atlanta, GA, 2022. https://research.gatech.edu/sites/default/files/inline-files/gt_epri_nox_emission_h2_short_paper.pdf.
(34) Skottene, M.; Rian, K. E. A study of NOx formation in hydrogen flames. *Int. J. Hydrogen Energy* **2007**, *32* (15), 3572−3585.
(35) Goswami, M.; et al. *Updated Kinetic Mechanism for NOx Prediction and Hydrogen Combustion*; Technical Report No. FP7-ENERGY-2008-TREN-1; Technische Universiteit Eindhoven: Eindhoven, The Netherlands, 2008. https://etn.global/wp-content/uploads/2019/02/WP1-1_Milestone2-2_TUe-Report.pdf.
(36) Leparoux, J.; Mercier, R.; Puggelli, S.; Cailler, M.; Moureau, V. Numerical Investigation of a Hydrogen−Air Flame for NOx Prediction. *J. Eng. Gas Turbines Power* **2024**, *146* (9), 091015.
(37) Capurso, T.; et al. NOx pathways in lean partially premixed swirling H2-air turbulent flame. *Combust. Flame* **2023**, *248*, 112581.
(38) Khateeb, A. A.; et al. Stability limits and NO emissions of premixed swirl ammonia-air flames enriched with hydrogen or methane at elevated pressures. *Int. J. Hydrogen Energy* **2021**, *46* (21), 11969−11981.
(39) Ditaranto, M.; Saanum, I.; Larfeldt, J. Experimental study on high pressure combustion of decomposed ammonia: How can ammonia be best used in a gas turbine? In *Turbo Expo: Power for Land, Sea, and Air*; American Society of Mechanical Engineers, 2021.
(40) Park, S. Hydrogen addition effect on NO formation in methane/air lean-premixed flames at elevated pressure. *Int. J. Hydrogen Energy* **2021**, *46* (50), 25712−25725.

https://doi.org/10.1021/acs.energyfuels.5c05963
Energy Fuels 2026, 40, 3806−3816